molecules

MDPI

Article

New Tricholomalides D–G from the Mushroom *Tricholoma ustaloides* Grown in an Italian Beech Wood

Gianluca Gilardoni [1], Francesca Negri [2], Paola Vita Finzi [2], Faiq H. S. Hussain [3] and Giovanni Vidari [2,3,*]

[1] Departamento de Química, Universidad Técnica Particular de Loja (UTPL), Loja 110107, Ecuador; ggilardoni@utpl.edu.ec or gianluca.gilardoni@gmail.com
[2] Dipartimento di Chimica, Università degli Studi di Pavia, Via Taramelli 10, 27100 Pavia, Italy; f.negri@mail.com (F.N.); paola.vitafinzi@unipv.it (P.V.F.)
[3] Department of Medical Analysis, Faculty of Applied Science, Tishk International University, Erbil 44001, Iraq; faiq.hussain@tiu.edu.iq
* Correspondence: vidari@unipv.it

Abstract: Four novel seconeodolastane diterpenoids, named tricholomalides D–G, were isolated, together with the known tricholomalide C, from the fruiting bodies of *Tricholoma ustaloides* Romagn., a species belonging to the large *Tricholoma* genus of higher mushrooms (*Basidiomycota*, family *Tricholomataceae*). They were isolated through multiple chromatographic separations, and the structures, including the absolute configuration, were established through a detailed analysis of MS, NMR, and CD spectral data and comparison with related compounds reported in the literature, which has been thoroughly revised.

Keywords: *Tricholoma ustaloides*; *Tricholomataceae* (*Basidiomycota*); seconeodolastane diterpenoids; tricholomalides; CD spectra; absolute configuration

Citation: Gilardoni, G.; Negri, F.; Vita Finzi, P.; Hussain, F.H.S.; Vidari, G. New Tricholomalides D–G from the Mushroom *Tricholoma ustaloides* Grown in an Italian Beech Wood. *Molecules* **2023**, *28*, 7446. https://doi.org/10.3390/molecules28217446

Academic Editors: Xing-De Wu and Zheng-Hong Pan

Received: 22 September 2023
Revised: 25 October 2023
Accepted: 3 November 2023
Published: 6 November 2023

1. Introduction

More than 250 species are included in the genus *Tricholoma* (Fr.) Staude [1], which is the largest in the family *Tricholomataceae* of the order *Agaricales* (*Basidiomycota*). The species have a worldwide distribution and are mainly found in temperate and subtropical zones in both the southern and northern hemispheres [2], from Australia and China to North America and Europe [3–8].

The use of molecular methods based on nuclear rDNA internal transcribed spacer ITS1-5.8S-ITS2 (ITS) sequences is becoming more and more important in phylogenetic studies of higher mushrooms [7–9], accompanying or even substituting the traditional studies of fungal morphological characters. Thus, it has often been demonstrated that mushrooms growing in different habitats/countries but classified as the same species based on morphological characters, must instead be placed in distinct clades/subclades or even different taxa [8,10,11]. In this context, the distinct chemical contents determined through phytochemical analysis have often confirmed the possible existence of different varieties or taxa [12].

Our interest in the chemical analysis of *Tricholoma* species grown in Italy was thus motivated by taxonomical reasons, as the morphological characters alone make it difficult to differentiate some species, e.g., those included in the section *Genuina* [7]. However, not less important was the fact that the fruiting bodies of most *Tricholoma* produce a wide variety of secondary metabolites, exhibiting unusual/rare structures and important biological activities, including cytotoxic and antimicrobial properties, neurite outgrowth stimulation effects, acetylcholinesterase inhibitory activity, etc. [13].

Continuing our studies on *Tricholoma* species grown in Italy, our attention was recently drawn to the phytochemical study of *Tricholoma ustaloides* Romagn. (Figure 1A), which has been included by Heilmann-Clausen and Christensen in the critical section *Genuina* [7].

This mushroom, which is considered inedible in Europe, is generally rare in Italy, where it typically grows from late summer to late autumn in association with oak, chestnut, hornbeam, and beech trees [4,5] (Figure 1B).

(**A**) (**B**)

Figure 1. Specimens of *Tricholoma ustaloides* (**A**) collected in a beech wood (**B**) in Northern Apennines near Pavia, Italy (photos provided by Teresio Restelli and Alfredo Gatti).

In our initial phytochemical investigation of an aqueous methanol sub-extract of an EtOAc extract of *T. ustaloides* fruiting bodies, we isolated two rare C-30 terpenoids, saponaceolides J (**1**) and F (**2**), three cyclic lactone-containing lanostane triterpenoids, tricholidic acid (**3**), the new tricholidic acids B (**4**) and C (**5**), and the rare tricholomenyn C (**6**) (Figure 2). In addition, mixtures of undetermined triglycerides and free fatty acids, together with five unidentified diterpenoids (A1–A5), were isolated [14].

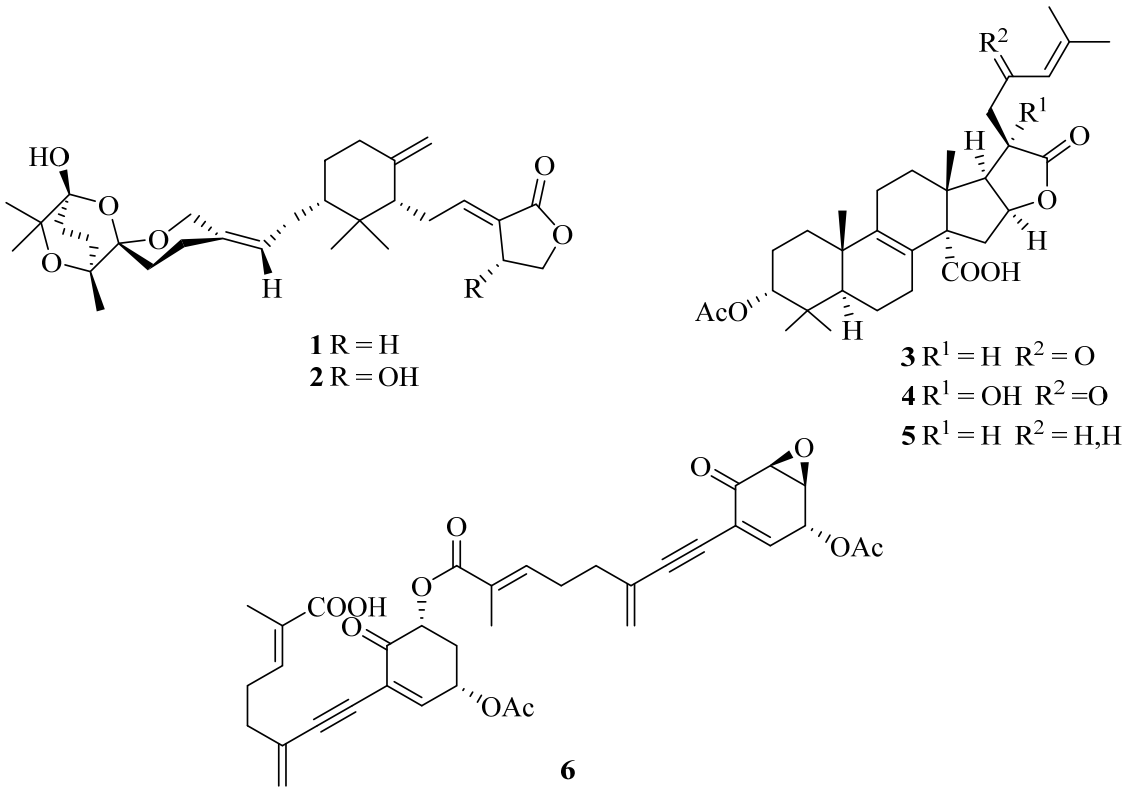

Figure 2. Structures of saponaceolides J (**1**) and F (**2**), tricholidic acid (**3**), tricholidic acids B (**4**) and C (**5**), and tricholomenyn C (**6**) isolated from *Tricholoma ustaloides*.

In this paper we report the structures of compounds A1–A5, which were established through interpretation of IR, MS, 1D, and 2D NMR spectral data. The assignment of the absolute configuration (AC) to these compounds was based on the interpretation of electronic circular dichroism (ECD) spectra. In general, determination of the absolute configuration of natural products using ECD compares the spectrum of a new compound having an unknown AC to those of analogous compounds of known ACs [15]. However, AC determination by predicting the sign of one or more bands in the ECD spectrum using empirical, semiempirical, or nonempirical rules is often an option [15,16]. Another widely used option is to compare calculated and experimental ECD spectra [15].

The assignment of stereostructures to the compounds A1–A5 heavily depended on those of related diterpenoids previously isolated from other *Tricholoma* species. Since there are several discrepancies in the literature about the structures of the latter compounds [13], especially about their ACs, the discussion of the structures of A1–A5 is preceded by a short critical review of the existing literature.

2. Diterpenoids Isolated from *Tricholoma* Fruiting Bodies: A Short Critical Review

Diterpenoids are a class of terpenes formally composed of four isoprene units, that are biosynthesized by plants, animals, and fungi, including higher mushrooms (*Basidiomycota*) [17], via the HMG-CoA reductase pathway, with geranylgeranyl pyrophosphate being a primary intermediate [18]. Only a few examples of diterpenoids have been isolated so far from fruiting bodies of *Tricholoma* [13].

2.1. Trichoaurantianolides and Tricholomalides

All the diterpenoids isolated from fruiting bodies of *Tricholoma* species have a rare rearranged terpenoid skeleton, which has been named seconeodolastane in accordance with the proposed biosynthetic pathway (vide infra, Scheme 1). They belong to two diastereomeric families, the trichoaurantianolides and the tricholomalides, respectively, depending on the stereochemistry of the OH group at the C-8 position of the seconeodolastane skeleton (vide infra).

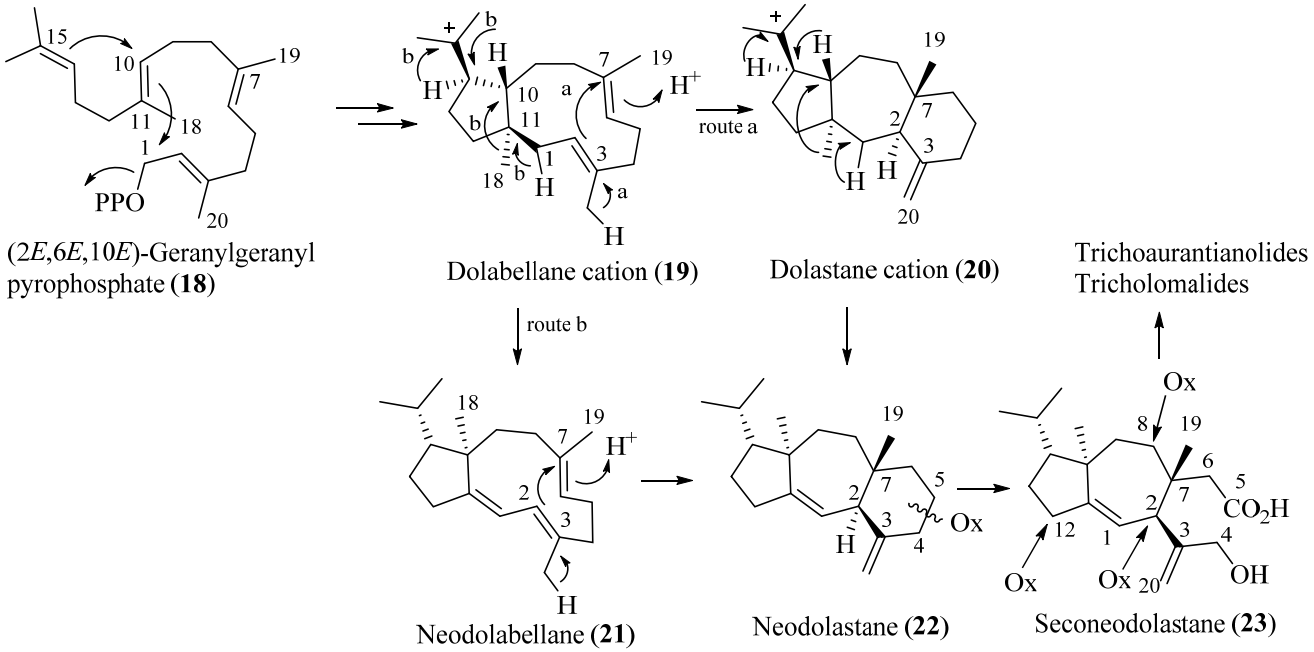

Scheme 1. Proposed biosynthetic pathways of trichoaurantianolides and tricholomalides.

The first group of diterpenoids includes trichoaurantianolides A–D (**7**–**10**), which were isolated from wild fruiting bodies of *T. aurantium* (Schaeff.: Fr.) Ricken collected

in Italy [19,20]; trichaurantin **8** (*synonym* of trichoaurantianolide B), which was isolated from the fruiting bodies of *T. aurantium* and *T. fracticum* (Britz.) Kreis. (syn. *T. batschii* Gulden) collected in Germany [21]; and acetyl trichaurantin (**11**), which was isolated from *T. aurantium* [21].

Structures **7**–**11** were established using 2D NMR data and using single-crystal X-ray analysis in the case of alcohol **8** [20,21]. Moreover, the absolute configurations of trichoaurantianolides B (**8**), C (**9**), and D (**10**) (Figure 3) were firmly established using anomalous X-ray diffraction and chemical interconversions [20,21], and enantioselective total synthesis [22]. Thus, the absolute stereochemistry of trichoaurantianolide C (**9**) was identical to the one initially assigned to this compound on the basis of the weak Cotton effect (CE) observed at 300 nm ($\Delta\varepsilon$ = +0.14) [20]. In fact, based on an empirical rule [16], the positive sign of the CE of compound **9**, for which the molecular modeling indicated a "twisted" conformation of the cyclopentanone ring, corresponded to the signs of the octants occupied by the carbons of the ring (see structure A in Figure 4). Instead, misapplication of the octant rule [16] to the positive CE of trichoaurantianolide C resulted in the erroneous assignment of the enantiomeric configuration *ent*-**9** (see structure *ent*-A in Figure 4) [23].

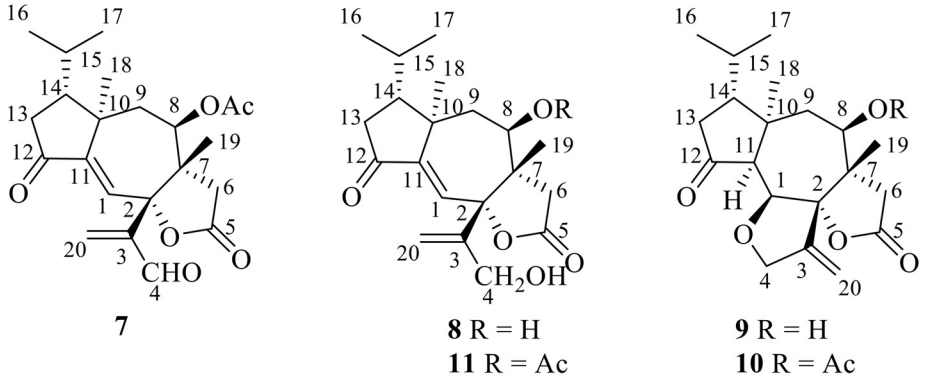

Figure 3. Structures of trichoaurantianolides A–D (**7**–**10**) and acetyl trichaurantin (**11**).

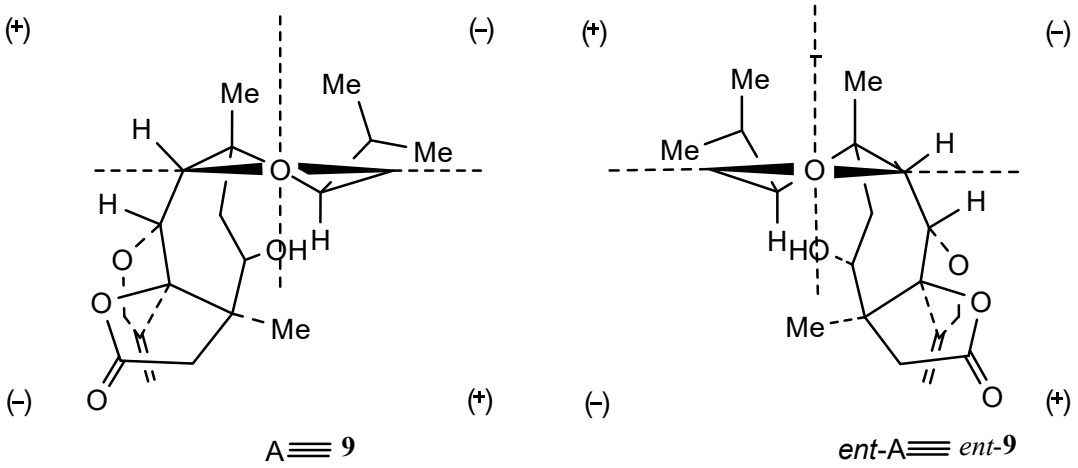

Figure 4. A: octan projections of the "twisted" conformation of the cyclopentanone ring in trichoaurantianolide C (**9**); B: octan projection of *ent*-**9**.

Tricholomalides A–C were isolated from the methanol extract of fresh fruiting bodies of an undetermined species of *Tricholoma* collected in Japan [23]. Noteworthily, these diterpenoids significantly induced neurite outgrowth in rat pheochromocytoma cells at concentrations of 100 μM [23]. The stereostructures of tricholomalides A–C, which were similar to those of trichoaurantianolides **7**–**11**, were definitely established as **12**–**14** (Figure 5)

using total synthesis and single-crystal X-ray diffraction. Thus, the stereochemistry at C-2 in tricholomalides A (**12**) and B (**13**) [24] was established to be opposite to the one originally assigned to these compounds based on spectral data only [23]. Moreover, H-8 was *cis* to H_3-19, while it was *trans* in compounds **7**–**11**.

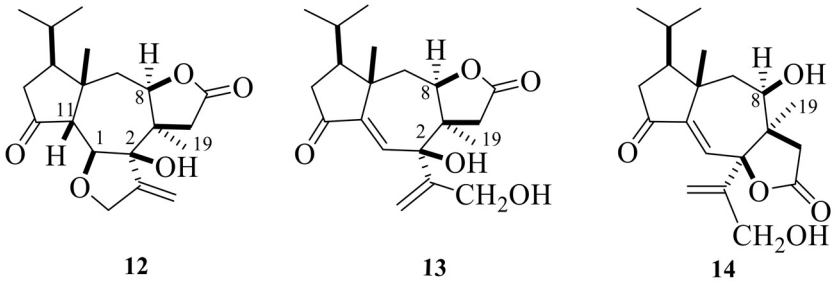

Figure 5. Structures of tricholomalides A–C [23,24].

The absolute configuration of tricholomalides A–C has not yet been determined unambiguously. However, biosynthetic considerations (vide infra, Scheme 1) and interpretation of the CD data applying the empirical rule of twisted cyclopentanones [16], instead of the octant rule used in the paper reporting the isolation of tricholomalides [23], have strongly suggested that the configuration is identical to that of trichoaurantianolides, thus inverting the original assignment [23]. In fact, like trichoaurantianolide C (**9**) [20], tricholomalide A (**15**) exhibited a positive Cotton effect at 302 nm ($\Delta\varepsilon$ + 0.31) [23], indicating a similar "positively twisted" conformation of the cyclopentanone ring (see the discussion above). In addition, tricholomalide B (**16**) was converted to **15** during storage at 4 °C in DMSO [23], and the CD spectra of the *cisoid* α,β-unsaturated ketones **16** and **17** revealed CEs with the same signs for the corresponding peaks at 250 ($\Delta\varepsilon$ − 0.57) and 336 nm ($\Delta\varepsilon$ + 0.53) for **16** and at 234 ($\Delta\varepsilon$ − 0.22) and 344 nm ($\Delta\varepsilon$ + 0.16) for **17** [23].

In summary, the absolute stereochemistry depicted in Figure 6 is proposed for tricholomalides A–C (**15**–**17**).

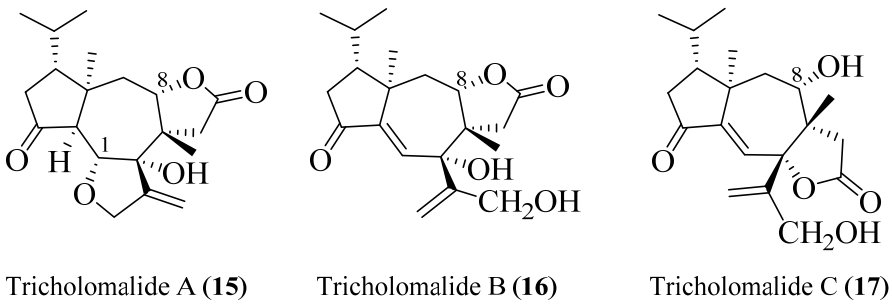

Figure 6. Absolute configurations proposed for tricholomalides A–C.

Biosynthetically, trichoaurantianolides and tricholomalides should originate from an enzymatically controlled stereoselective cyclization of geranylgeranyl pyrophosphate (**18**) producing nonracemic dolabellane cation **19**. This intermediate would be the precursor of the dolastane (**20**), neodolabellane (**21**), and neodolastane (guanacastane) (**22**) skeletons through a series of stereospecific transannular cyclizations and Wagner–Meerwein migrations (Scheme 1). The seconeodolastane skeleton (**23**) of trichoaurantianolides and tricholomalides would finally result from oxidation and cleavage of the six-membered ring in **22** (Scheme 1), while oxidative decoration of the structures at C-2, C-8, and C-12 would likely occur in the latest steps of the biosynthetic path to trichoaurantianolides and tricholomalides. It is interesting to note that diterpenoids originating from a common biogenetic pathway in algae, fungi, liverworts, and higher plants are enantiomeric to the corresponding metabolites isolated from species of marine invertebrates [13,25].

3. Results and Discussion

3.1. Tricholomalides from Tricholoma Ustaloides

In the following paragraphs, we will describe the determination of the structures of compounds A1–A5, whose isolation from *T. ustaloides* fruiting bodies was reported in a recent paper [14]. A1–A4 were new diterpenoids, named tricholomalides D–G (**24**–**27** in Figure 7), respectively, while A5 was identified as the known tricholomalide C (**17**) [23]. At first, we will discuss the structures of tricholomalides D (**24**), E (**25**), and G (**27**), which showed a γ-lactone ring *cis*-fused at C-2 and C-7 with the central cycloheptene ring of the seconeodolastane skeleton. Subsequently, we will describe the structure of tricholomalide F (**26**), in which the γ-lactone ring is *cis*-fused with the cycloheptene ring at C-7 and C-8.

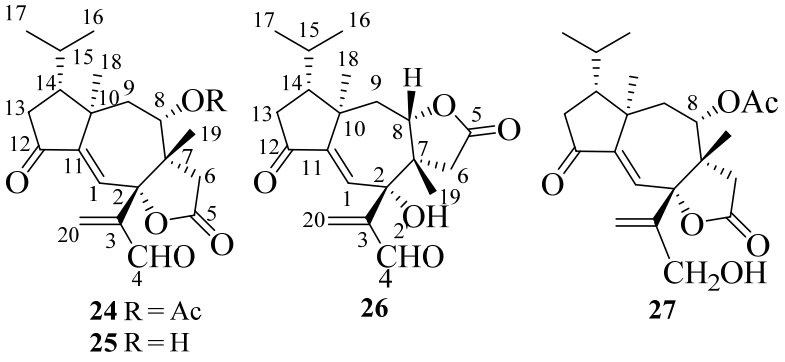

Figure 7. Structures of tricholomalides D–G (**24**–**27**).

3.1.1. Tricholomalides C, D, E, and G

The molecular formula of tricholomalide D (**24**) was established as $C_{22}H_{28}O_6$ by EIMS (Figure S9 in the Supplementary Materials), elemental analysis, and ^{1}H and ^{13}C NMR spectra (Table S1 in the Supplementary Materials). It indicated nine degrees of unsaturation. The oxygen-containing functionalities in the molecule were established as one cyclopentanone (C-12), one formyl (C-4), one γ-lactone (C-5), and one acetoxy (C-21) group from the IR bands (1783, 1736, 1699 cm^{-1}) and the characteristic chemical shifts (δ_C 205.0, 191.8, 175.2, and 169.4 ppm, respectively) of the corresponding carbonyl carbons in the ^{13}C NMR spectrum (Figures S7 and S8 in the Supplementary Materials).

The NMR spectra of compound **24** (Figures S5 and S7 and Table S1 in the Supplementary Materials) showed signals for one trisubstituted (δ_C 125.9 (d, C-1) and 151.3 (s, C-11); δ_H 6.63 (1H, s, H-1)) and one *exo*-methylene double bond (δ_C 138.4 (t, C-20) and 148.6 (s, C-3); δ_H 6.41 (1H, br s, H_Z-20) and 6.62 (1H, br s, H_E-20)). HMBC correlations (Figure 8A) indicated that the two olefins were α,β-conjugated to the ketone (C-12) and the aldehyde (C-4) groups, respectively, while they were bound to each other through an oxygenated quaternary carbon placed in the lactone ring (δ_C 87.4 (s, C-2)). The remaining two unsaturations of tricholomalide D (**24**) were then assigned to two rings that formed a tricyclic carbon skeleton together with the γ-lactone. The ^{1}H NMR spectrum of **24** (Figure S5 in the Supplementary Materials) showed two methyl singlets at δ_H 0.98 (H_3-19) and 1.12 (H_3-18) that were attached to quaternary carbons C-7 (δ_C 49.8 s) and C-10 (δ_C 44.7 s), respectively, and two methyl doublets of an isopropyl group at δ_H 0.95 (J = 6.5 Hz, H_3-17) and 1.02 (J = 6.5 Hz, H_3-16). The remaining proton and carbon atoms of compound **24** were assigned to three separate moieties, I–III based on ^{1}H-^{1}H COSY data (Figure S6 in the Supplementary Materials) and selective homonuclear decoupling experiments. The moiety I linked C-13 to C-16 and included the H-15 (δ_H 1.75–1.85, 1H, m) to H_3-17 linkage. The spin system of the unit II was an isolated AB quartet (δ_H 2.29 and 2.88, 2H, J_{AB} = 18.5 Hz), which was assigned to an isolated methylene (H_2-6) attached to the γ-lactone carbonyl group (δ_C 175.2, s, C-5) by HMBC correlations (Figure 8A). The moiety III gave rise to a distorted AMX system which includes a methylene (H_2-9; δ_H 1.79 (1H, dd, 15.0, 11.5) and δ_H 2.15 (1H,

dd, 15.0, 2.0)) and a methine hydrogen (H-8; δ_H 4.72 (1H, ddd, 11.5, 2.0, 1.0)). This proton was geminal to the acetoxy carbonyl carbon (δ_C 169.4, s, C-21) via an HMBC cross peak with C-21 (Figure 8A). Assembling these partial structures using the two- and three-bond C-H connectivity data from HMBC correlations (Figure 8A), we unambiguously assigned structure **24** to tricholomalide D. The structure of the ring system was determined by (i) the bonds around the angular methyl (H_3-19) attached to C-7 (δ_C 49.8 s), which linked C-6 (δ_C 35.3 t) and C-9 (δ_C 37.7 t) to C-19 (δ_C 22.4 q) via C-7 and C-8 (δ_C 74.4 d); (ii) the linkages from H_3-19, H_2-20, and H-4 (δ_H 9.70 (1H, s)) to C-2 (δ_C 87.4 s) and those from H-1 (δ_H 6.63 (1H, s)) to C-2, thanks to which the acrolein moiety was connected to C-2 and the arrangement of the substituents of the γ-lactone ring was defined; (iii) the connectivities from H_3-18 to C-10 (δ_C 44.7 s), C-9 and C-11 (δ_C 151.3 s), and H-1 to C-10, of which C-12 and C-2 indicated the presence of a cycloheptene ring bearing an angular methyl (H_3-18) on an allylic sp^3 quaternary carbon (C-10); (iv) the linkage of the isopropyl group to C-18 (δ_C 21.4 q) via C-14 (δ_C 47.2 d), which defined the placement of the moiety I to form a cyclopentanone ring. These data and 1D NOE correlations (Figure 8B), H-15/H_3-18; H_3-18/H-9α; H-8/H-9β and H-8/H_3-19; H_3-19/H-6β, H-4/H_3-19, and H-6β/H-20*E* (Figure 8B), suggested that tricholomalide D (**24**) was the C-8 epimer of trichoaurantianolide A (**7**) [19]. Thus, the 8-acetoxy group was *trans* to H_3-19 in **24**, while it was *cis* in **7** [19]. This finding was confirmed by the significantly different chemical shift and coupling constants of H-8 in **24** (δ_H 4.72; $J_{8\beta\text{-}9\beta}$ = 2.0 and $J_{8\beta\text{-}9\alpha}$ = 11.5 Hz) and in **7** (δ_H 5.15; $J_{8\alpha\text{-}9\beta}$ = 9.5 and $J_{8\alpha\text{-}9\alpha}$ = 1.5 Hz) [19].

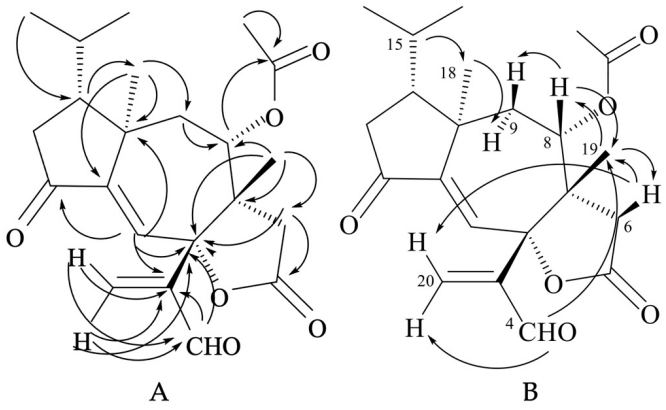

Figure 8. HMBC (H → C) correlations (**A**) and 1D NOE correlations (H → H) (**B**) observed for tricholomalide D (**24**).

The molecular formula of tricholomalide E (**25**), $C_{20}H_{26}O_5$, was established from the EIMS (Figure S15 in the Supplementary Materials) and the ^{1}H and ^{13}C NMR spectra (Figures S11–S14 in the Supplementary Materials). The NMR spectral data (Table S1 in the Supplementary Materials) clearly indicated that it was the deacetyl derivative of tricholomalide D (**24**). In fact, the signals of an acetyl group were missing in the ^{1}H and ^{13}C NMR spectra of **25** (Figures S11 and S13 in the Supplementary Materials), while the signals of H-8 (δ_H 3.63, br d, 11.5) and C-8 (δ_C 71.6 d) in the ^{1}H and ^{13}C NMR spectra, respectively, of alcohol **25** moved upfield by about 1 and 3 ppm, respectively, in comparison with the corresponding signals of the acetate **24** (vide supra). Finally, the structure of **25** was confirmed with standard acetylation with Ac_2O/Py, which afforded a product that was identical with acetate **24**.

Tricholomalide G (**27**), with the molecular formula $C_{20}H_{26}O_5$ from the EIMS (Figure S27 in the Supplementary Materials) and the ^{1}H and ^{13}C NMR spectra (Figures S23–S26 in the Supplementary Materials), was identified as the dihydroderivative of aldehyde **24** through the following significant differences between the NMR spectra of the two compounds (Figures S23–S26 and Table S1 in the Supplementary Materials): (i) the presence of two diastereotopic protons (H_2-4) at δ_H 4.22 (1H, dd, 13.0, 1.1) and 4.27 (1H, br d, 13) in the ^{1}H

NMR spectrum of **27**, assignable to an allylic CH_2OH group, which replaced the signal H-4 (δ_H 9.70 (1H, s)) of aldehyde **24**; (ii) the upfield shift of the H_2-20 protons (δ_H 5.32 (1H, s) and δ_H 5.67 (1H, t, 1.1)) and the C-20 carbon (δ_C 118.3, t), respectively, in the ^{1}H and ^{13}C NMR spectra of **27**, compared with the corresponding signals of the βCH_2 group of the acrolein moiety in **24**. Finally, the structure of compound **27** was confirmed through the oxidation of the allylic alcohol with PDC (pyridinium dichromate), which afforded a product indistinguishable from aldehyde **24**.

The NMR spectral data (Figures S1–S3 in the Supplementary Materials) and the signs of the CD maxima of compound A5 (Figure S4 in the Supplementary Materials) were identical with the data reported in the literature for tricholomalide C (**17**) [23]. Moreover, selective oxidation of A5 (≡**17**) with PDC gave a product indistinguishable from aldehyde **25**.

3.1.2. Tricholomalide F

Tricholomalide F (**26**) possessed the same molecular formula as tricholomalide E (**25**), $C_{20}H_{26}O_5$, as inferred from the EIMS spectrum (Figure S21 in the Supplementary Materials) and the ^{1}H and ^{13}C NMR spectral data (Figures S17–S20 and Table S2 in the Supplementary Materials). These data resembled those reported for tricholomalide B (**16**) [23], except for the presence of a formyl group (H_4 (δ_H 9.55, 1H, s) and a C-4 carbonyl group (δ_C 196.3, d)) bound to C-3 (δ_C 148.6 s) in **26** which replaced the allylic CH_2OH group occurring in compound **16** [23]. The presence of a free tertiary OH group attached to C-2 of **26** was revealed by the singlet at δ_C 76.1 in the ^{13}C NMR spectrum (Figure S19 in the Supplementary Materials), while the signals of H-8 (δ_H 3.92, 1H, dd, 12.8, 2.5) and C-8 (δ_C 85.0, d) in the NMR spectra of **26** (Figures S17 and S19 in the Supplementary Materials) indicated the ring closure of the γ-lactone unit on C-8.

The two- and three-bond HMBC correlations (Figure 9A) were fully consistent with the gross structure of **26**, while the relative stereochemistry of the stereogenic carbons in **26** was established through selective 1D NOE experiments (Figure 9B). In fact, the correlations of H-15 (δ_H 1.75–1.92 (1H, m)) with H_3-18 (δ_H 1.20 (3H, s)) and between H_3-18 and H-9α (δ_H 2.79 (1H, dd, 14.0, 12.8)) indicated that the isopropyl group, H_3-18, and H-9α were oriented on the same side of the tricyclic structure, while the interactions of H-8 with H-9β (δ_H 2.23 (1H, dd, 14.0, 2.5)) and H_3-19 (δ_H 0.97 (3H, br s)) and H-4 with H_3-19 (Figure 9B) revealed that they were placed on the opposite sides of H_3-18 and H-9α. The resulting stereochemistry of compound **26** was further corroborated by the J = 12.8 Hz of H-8β with H-9α and by the NOE interactions of H-8β with H-6β (δ_H 1.86 (1H, d, 17.0)) and H-6α (δ_H 3.24 (1H, dd, 17.0, 1.0)) with 2-O*H* (δ_H 4.92 (1H, d, 1.0)). Interestingly, H-1 (δ_H 6.97 (1H, d, 1.0)) was coupled with 2-O*H* by a J_W coupling of 1 Hz, which indicated a rather rigid orientation of the tertiary hydroxy group.

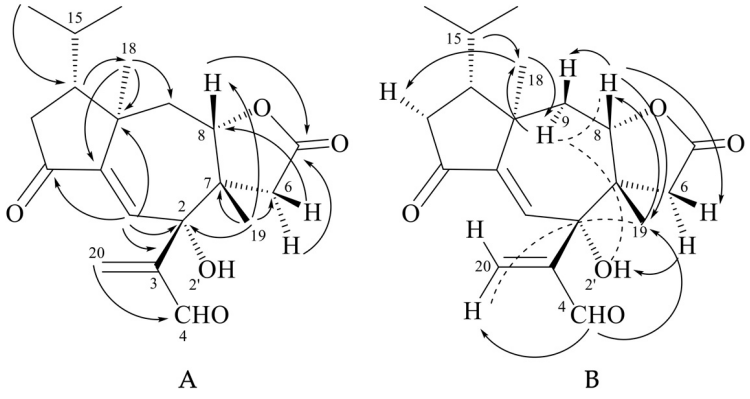

Figure 9. (**A**) HMBC (H → C) correlations; (**B**) 1D NOE correlations (H → H) observed for tricholomalide F (**26**); ⟶ strong NOE effect; ⇢ weak NOE effect.

In summary, tricholomalides D–G (**24**–**27**) exhibited a relative stereochemistry identical to that of tricholomalides B (**16**) and C (**17**), while they were epimers of trichoaurantianolides at C-8.

3.1.3. Absolute Configuration of Tricholomalides D–G

The absolute configuration of tricholomalides D–G (**24**–**27**) shown in Figure 7 was established on the basis of chemical interconversions, biosynthetic considerations (see above), and CD data (Figures S10, S16, S22 and S28 in the Supplementary Materials). The *cisoid* α,β-unsaturated cyclopentanone system occurring in **24**–**27** is also a characteristic feature of the structures of tricholomalides B (**16**) and C (**17**), as well as of trichoaurantianolides **7**, **8**, and **11**, whose configuration was thoroughly discussed in a previous Section 2.1. All the CD spectra of these compounds revealed Cotton effects with positive signs for the respective peaks in the region of 300–350 nm (Figures S10, S16, S22 and S28 in the Supplementary Materials), which were thus closely associated with similar conformational and dissymmetric substituent effects on the *cisoid* α,β-unsaturated ketone unit. Therefore, tricholomalides D–G (**24**–**27**) were assigned the same absolute configuration as tricholomalides B (**16**) and C (**17**) (Figures 6 and 7), having a stereochemistry at C-8 that was opposite to that determined for trichoaurantianolides **7**, **8**, and **11** (Figure 3). This finding is not unexpected, as the configurations at C-7, C-10, and C-14 arise from stereospecific transannular cyclizations and Meerwein–Wagner rearrangements in the first steps of the common biosynthetic path leading to the tricholomalides and trichoaurantianolides (Scheme 1). Instead, the hydroxylation at C-8 likely involved a neodolastane or seconeodolastane derivative at a late step of the biosynthetic path, and it was controlled by enzymes with opposite diastereoselectivities for tricholomalides and trichoaurantianolides, respectively.

4. Materials and Methods

4.1. General Experimental Techniques and Procedures

Preparative chromatographic separations were carried out on open columns at atmospheric pressure (CC). The columns were manually packed with silica gel (Merck Kieselgel 60, 40–63 μm, Rahway, NJ, USA) or reversed-phase C_{18} (Merck LiChroprep RP-18, 25–40 μm) purchased from Sigma-Aldrich (St. Louis, MO, USA). Thin-layer chromatographic (TLC) analyses were conducted over glass-supported silica gel 60 (0.25 mm; GF_{254}, Merck) or RP-18 (F254s, Merck) plates (Sigma-Aldrich). Spots on TLC plates were initially visualized under UV light (254 and 366 nm); subsequently, they were sprayed with a 0.5% solution of vanillin in H_2SO_4/ethanol 4:1 and finally heated with a hot gun until reaching maximum color development. Semipreparative medium-pressure liquid chromatographic (MPLC) separations were performed with an Isolera instrument (Biotage, Uppsala, Sweden) equipped with silica gel and RP-18 reversed-phase cartridges and a dual-wavelength UV detector. Reagent-grade solvents, purchased from Carlo Erba (Milan, Italy) or from Aldrich, were used for extraction and chromatographic separations. Optical rotation was conducted using PerkinElmer 241 polarimeter (Walthman, MA, USA); CD spectra were obtained using Jasco J-1500 CD spectrometer (Tokyo, Japan) in MeOH. IR spectra were obtained using PerkinElmer Paragon 100 PC FT-IR spectrometer (Walthman, MA, USA) on KBr disks. NMR spectra were obtained using Bruker AV300 and 400 spectrometers at 300 and 400 MHz (^{1}H), respectively, and at 75.47 and 100 MHz (^{13}C), respectively, operating at 22 °C (Billerica, MA, USA). ^{1}H NMR and ^{13}C NMR chemical shifts are relative to signals of residual $CHCl_3$ (δ_H 7.25, singlet) and $^{13}CDCl_3$ δ_C (77.0, central line of a triplet) in $CDCl_3$ (Sigma-Aldrich, Steinheim, Germany); coupling constants (*J*) were measured in Hz; multiplicity (=number of attached hydrogens) of each C-atom was determined using DEPT experiments; COSY, DEPT, and HSQC spectra and NOE effects were recorded using standard pulse sequences. EIMS and DCI-MS (NH_3) spectra were obtained using Finnigan-MAT 822 mass spectrometer.

4.2. Fungal Material

The fruiting bodies of *Tricholoma ustaloides* Romagn. were collected in a beech wood at the end of September—beginning of October 2021 and identified by Alfredo Gatti, as reported in the inaugural study of this mushroom [14]. A sample specimen (accession code: TU001) was deposited at the Department of Chemistry, University of Pavia, Italy.

4.3. Extraction and Isolation

Extraction of the fresh fruiting bodies (990 g) with EtOAc, evaporation of the extract, and partition of the resulting residue between MeOH-H_2O at 90:10 and hexane were described in a previous paper [14]. The residue (2.8 g) from the aqueous methanol layer was subjected to multiple separations using semipreparative MPLC silica gel and RP-18 columns to afford compounds A1–A5, named tricholomalides D (**24**, 51 mg, 0.0051% on fresh fruiting bodies), E (**25**, 18.6 mg, 0.0019%), F (**26**, 5.5 mg, 0.0006%), G (**27**, 15.2 mg, 0.0015%), and C (**17**, 13.6 mg, 0.0014%), respectively [14].

4.3.1. Tricholomalide C (**17**)

Colorless, sticky oil; $[\alpha]_D^{22}$ + 32.9 (*c* 10.1 mg/mL, CH_2Cl_2); R_f 0.77 (RP18 TLC; MeOH-H_2O, 6:1); CD (MeOH) $\Delta\varepsilon_{236}$ −0.61, $\Delta\varepsilon_{345}$ +0.51; ^{1}H NMR (300 MHz, $CDCl_3$) δ_H 0.98 (3H, d, 6.5, H_3-17), 1.07 (3H, d, 6.5, H_3-16), 1.14 (3H, s, H_3-19), 1.16 (3H, s, H_3-18), 1.68-1.89 (2H, m, H-14 and H-15), 1.84 (1H, dd, 15.5 and 11.5, H_α-9), 2.11 (1H, dd, 15.5 and 2.0, H_β-9), 2.14 (1H, dd, 18.5 and 12.5, H_α-13), 2.37 (1H, dd, 18.0 and 1.0, H_β-6), 2.47 (1H, dd, 18.5 and 8.0, Hβ-13), 2.84 (1H, d, 18.0, Hα-6), 3.48 (1H, ddd, 11.5, 2.0, and 1.0, H-8), 4.21 (2H, br s, H_2-4), 5.30 (1H, s, H_Z-20), 5.63 (IH, s, H_E-20), 6.62 (1H, s, H-1); ^{13}C NMR (75.5 MHz, $CDCl_3$) δ_C 21.2 (q, C-18), 21.7 (q, C-17), 21.8 (q, C-19), 24.0 (q, C-16), 28.5 (d, C-15), 34.2 (t, C-6), 39.6 (t, C-9), 41.2 (t, C-13), 44.6 (s, C-10), 49.0 (d, C-14), 50.2 (s, C-7), 63.2 (t, C-4), 72.2 (d, C-8), 88.9 (s, C-2), 117.7 (t, C-20), 128.4 (d, C-1), 148.0 (s, C-3), 151.4 (s, C-11), 176.8 (s, C-5), 205.4 (C-12); IR (film): $\bar{\nu}_{max}$ 3425, 2969, 1758, 1726, 1647, 1461, 1246, 1199, 1020, 907 cm^{-1}; EIMS *m*/*z* (relative intensity) 348 $[M]^+$ $(C_{20}H_{28}O_5)^+$ (6), 333 $[M\text{-}CH_3]^+$ (46), 263 (100), 175 (21), 167 (59), 139 (23), 109 (25), 97 (39), 83 (21), 69 (50), 55 (36), 41 (60). Anal. Calcd for $C_{20}H_{28}O_5$: C, 68.94; H, 8.10. Found: C, 69.15; H, 8.18.

4.3.2. Tricholomalide D (**24**)

Colorless, sticky oil; $[\alpha]_D^{22}$ + 31.2 (*c* 10.9 mg/mL, CH_2Cl_2); R_f 0.53 (silica gel TLC; CH_2Cl_2-Me_2CO, 30:1); CD (MeOH) $\Delta\varepsilon_{220}$ −0.45, $\Delta\varepsilon_{246}$ +0.34, $\Delta\varepsilon_{350}$ +0.11; ^{1}H and ^{13}C NMR spectral data, see Table S1 in the Supplementary Materials; IR (film): $\bar{\nu}_{max}$ 2968, 1783, 1736, 1699, 1648, 1367, 1241, 1027, 990, 961 cm^{-1}; EIMS *m*/*z* (relative intensity) 388 $[M]^+$ $(C_{22}H_{28}O_6)^+$ (54), 359 $[M\text{-}CHO]^+$ (11), 346 $[M\text{-}CH_2CO]^+$ (18), 328 $[M\text{-}AcOH]^+$ (34), 313 (12), 285 (45), 269 (21), 263 (33), 178 (23), 163 (48), 133 (37), 106 (78), 95 (33), 83 (42), 69 (35), 58 (69), 43 (100). Anal. Calcd for $C_{22}H_{28}O_6$: C, 66.02; H, 7.27. Found: C, 66.15; H, 7.44.

4.3.3. Tricholomalide E (**25**)

Colorless, sticky oil; $[\alpha]_D^{22}$ + 1.2 (*c* 5.2 mg/mL, CH_2Cl_2); R_f 0.67 (RP18 TLC; MeOH-H_2O, 80:20); CD (MeOH) $\Delta\varepsilon_{225}$ −2.28, $\Delta\varepsilon_{246}$ +0.11, $\Delta\varepsilon_{272}$ −0.68, $\Delta\varepsilon_{350}$ +0.46; ^{1}H and ^{13}C NMR spectral data, see Table S1 in the Supplementary Materials; IR (film): $\bar{\nu}_{max}$ 3474, 2929, 1780, 1723, 1696, 1647, 1461, 1375, 1246, 1024, 962 cm^{-1}; EIMS *m*/*z* (relative intensity) 346 $[M]^+$ $(C_{20}H_{26}O_5)^+$ (31), 287 (40), 263 (58), 231 (22), 203 (22), 191 (36), 173 (25), 167 (82), 163 (51), 151 (37), 133 (39), 121 (30), 109 (32), 91 (40), 83 (61), 69 (68), 55 (68), 43 (100). Anal. Calcd for $C_{20}H_{26}O_5$: C, 69.34; H, 7.57. Found: C, 69.75; H, 7.78.

4.3.4. Tricholomalide F (**26**)

Colorless, sticky oil; $[\alpha]_D^{22}$ + 63.9 (*c* 1.8 mg/mL, CH_2Cl_2); R_f 0.57 (RP18 TLC; MeOH-H_2O, 80:20); CD (MeOH) $\Delta\varepsilon_{255}$ +0.47, $\Delta\varepsilon_{275}$ −0.05, $\Delta\varepsilon_{340}$ +0.20; ^{1}H and ^{13}C NMR spectral data, see Table S2 in the Supplementary Materials; IR (film): $\bar{\nu}_{max}$ 3561, 3416, 2941, 2876, 1783, 1765, 1725, 1638, 1461, 1371, 1242, 1051, 976 cm^{-1}; EIMS *m*/*z* (relative intensity) 346

$[M]^+$ $(C_{20}H_{26}O_5)^+$ (30), 331 $[M\text{-}CH_3]^+$ (9), 317 $[M\text{-}CHO]^+$ (33), 303 (35), 287 (23), 263 (99), 235 (46), 203 (29), 191 (61), 175 (27), 163 (61), 149 (43), 135 (48), 121 (33), 109 (38), 97 (47), 83 (58), 69 (84), 55 (88), 43 (70), 41 (100). Anal. Calcd for $C_{20}H_{26}O_5$: C, 69.34; H, 7.57. Found: C, 69.65; H, 7.73.

4.3.5. Tricholomalide G (**27**)

Colorless, sticky oil; $[\alpha]_D^{22}$ + 55.2 (*c* 4.8 mg/mL, CH_2Cl_2); R_f 0.57 (RP18 TLC; MeOH-H_2O, 80:20); CD (MeOH) $\Delta\varepsilon_{250}$ +0.43, $\Delta\varepsilon_{345}$ +0.18; ^1H and ^{13}C NMR spectral data, see Table S1 in the Supplementary Materials; IR (film): $\bar{v}_{max}$ 3449, 3060, 2960, 2929, 1772, 1731, 1644, 1463, 1370, 1241, 1020, 963, 938, 735 cm^{-1}; EIMS *m*/*z* (relative intensity) 390 $[M]^+$ $(C_{22}H_{30}O_6)^+$ (9), 375 $[M\text{-}CH_3]^+$ (54), 315 $[M\text{-}AcOH]^+$ (15), 263 (45), 191 (17), 181 (24), 167 (32), 135 (15), 109 (16), 95 (24), 69 (39), 55 (27), 43 (100), 41 (44). Anal. Calcd for $C_{22}H_{30}O_6$: C, 67.67; H, 7.74. Found: C, 67.81; H, 7.62.

*4.4. Acetylation of Tricholomalide E (**25**) to Tricholomalide D (**24**)*

Tricholomalide E (**25**) (3 mg, 8.7 μmol) in CH_2Cl_2 (1 mL) was added to pyridine (50 μL), followed by excess Ac_2O (50 μL). The mixture was stirred for 2 h at 22 °C, quenched with MeOH (0.5 mL), and evaporated. The residue was filtered through a short pad of silica gel (300 mg). Elution with CH_2Cl_2-MeOH at 99:1 gave a product (3.3 mg, 99%) identical ($[\alpha]_D^{22}$, NMR data) to tricholomalide D (**24**).

*4.5. Oxidation of Tricholomalide G (**27**) to Tricholomalide D (**24**) and Tricholomalide C (**17**) to Tricholomalide E (**25**)*

Freshly prepared PDC (9 mg, 24 μmol) [26] was added in one portion to tricholomalide G (**27**) (3 mg, 7.7 μmol) dissolved in CH_2Cl_2 (0.5 mL). The mixture was stirred for 6 h at 22 °C; subsequently, it was diluted with abundant Et_2O. The organic layer was washed with aqueous $NaHCO_3$, dried (Na_2SO_4), and evaporated. The residue was filtered through a short pad of silica gel (300 mg). Elution with CH_2Cl_2-MeOH at 99:1 gave a product (2.3 mg, 77%) identical ($[\alpha]_D^{22}$, NMR data) to tricholomalide D (**24**).

Isolated tricholomalide C (**17**) was converted to tricholomalide E (**25**) in 75% yield using the procedure described above.

5. Conclusions

The isolation of four novel seconeodolastane diterpenoids, tricholomalides D–G, from *T. ustaloides* has confirmed that the fruiting bodies of *Tricholoma* mushrooms are rich sources of new compounds, most of which have unique chemical structures. The rare seconeodolastane skeleton of tricholomalides seems to be a characteristic feature of the diterpenoids present in the fruiting bodies of *Tricholoma*; however, epimeric derivatives, e.g., compounds **7** and **24**, are produced by different species, and this finding may be chemotaxonomically significant. So far, besides being isolated from fruiting bodies of the genus *Tricholoma*, seconeodolastane diterpenoids have only been isolated from a mycelial culture of *Lepista sordida* [27]. Interestingly, the genera *Tricholoma* and *Lepista* both belong to the family *Tricholomataceae* (*Agaricales*).

In the future, we will extend our investigations to the chemical contents of other *Tricholoma* species grown in the Italian woods, and, regarding tricholomalides C–G, we intend to study their biological activities using in vitro tests.

Supplementary Materials: The following supporting information can be downloaded at https://www.mdpi.com/article/10.3390/molecules28217446/s1: ^1H NMR graphical spectra of tricholomalides C–G; COSY graphical spectra of tricholomalides D–G; ^{13}C NMR graphical spectra of tricholomalides C–G; DEPT ^{13}C NMR graphical spectra of tricholomalides C–G; EIMS graphical spectra of tricholomalides D–G; CD graphical spectra of tricholomalides C–G; tabulated NMR spectral data of tricholomalides D–G.

Author Contributions: Conceptualization, G.V. and F.H.S.H.; investigation, F.N. and G.G.; writing—original draft preparation, F.N. and G.V.; writing—review and editing, G.V.; supervision, G.V. and P.V.F. All authors have read and agreed to the published version of the manuscript.

Funding: This research received no external funding.

Institutional Review Board Statement: Not applicable.

Informed Consent Statement: Not applicable.

Data Availability Statement: Raw data are available from one of the authors (G.V.).

Acknowledgments: We are grateful to the Universidad Técnica Particular de Loja (UTPL) for supporting open access publication. We warmly thank Alfredo Gatti (Gruppo Micologico Vogherese) for the mushroom identification and the wood picture in Figure 1, and Teresio Restelli (Gruppo Micologico Pavese) for the mushroom picture in Figure 1.

Conflicts of Interest: The authors declare no conflict of interest.

References

1. Staude, F. *Die Schwämme Mitteldeutschlands, insbesondere des Herzogthums Coburg*; Dietz: Hannover, Germany, 1857.
2. Tedersoo, L.; May, T.W.; Smith, M.E. Ectomycorrhizal lifestyle in fungi: Global diversity, distribution, and evolution of phylogenetic lineages. *Mycorrhiza* **2010**, *20*, 217–263. [CrossRef]
3. Bessette, A.E.; Bessette, A.R.; Roody, W.C.; Trudell, S.A. *Tricholomas of North America: A Mushroom Field Guide*; University of Texas Press: Austin, TX, USA, 2013; p. 1.
4. Bon, M. *Champignons de France et d'Europe Occidentale*; Flammarion: Paris, France, 2004.
5. Riva, A. *Tricholoma (Fr.) Staude. Fungi Europaei*; Candusso Editrice: Origgio, Italy, 2003; Volume 3, ISBN 88-901057-1-2A.
6. Christensen, M.; Heilmann-Clausen, J. *The Genus Tricholoma. Fungi of Northern Europe*; Svampetrik: Tilst, Denmark, 2013; Volume 4.
7. Heilmann-Clausen, J.; Christensen, M.; Frøslev, T.G.; Kjøller, R. Taxonomy of *Tricholoma* in northern Europe based on ITS sequence data and morphological characters. *Persoonia* **2017**, *38*, 38–57. [CrossRef]
8. Reschke, K.; Popa, F.; Yang, Z.L.; Kost, G. Diversity and taxonomy of *Tricholoma* species from Yunnan, China, and notes on species from Europe and North America. *Mycologia* **2018**, *110*, 1081–1109. [CrossRef]
9. Cui, Y.Y.; Ding, X.X.; Kost, G.; Yang, Z.L. *Tricholoma* sect. *Tricholoma* (*Tricholomataceae*) from China: Molecular phylogeny and taxonomy. *Mycol. Prog.* **2022**, *21*, 35. [CrossRef]
10. Yang, Z.L.; Ding, X.-X.; Kost, G.; Rexer, K.-H. New species in the *Tricholoma pardinum* complex from Eastern Himalaya. *Phytotaxa* **2017**, *305*, 1–10. [CrossRef]
11. Aoki, W.; Endo, N.; Ushijima, S.; Nagai, H.; Ito, T.; Fukuda, M.; Yamada, A. Taxonomic revision of the Japanese *Tricholoma ustale* and closely related species based on molecular phylogenetic and morphological data. *Mycoscience* **2021**, *62*, MYC548. [CrossRef]
12. Clericuzio, M.; Hussain, F.H.S.; Amin, H.I.M.; Salis, A.; Damonte, G.; Pavela, R.; Vidari, G. New acetylenic metabolites from the toxic mushroom *Tricholoma pardinum*. *Nat. Prod. Res.* **2021**, *35*, 5081–5088. [CrossRef]
13. Clericuzio, M.; Mellerio, G.G.; Vita Finzi, P.; Vidari, G. Secondary metabolites isolated from *Tricholoma* species (*Basidiomycota*, Tricholomatacee): A review. *Nat. Prod. Commun.* **2018**, *13*, 1213–1224.
14. Gilardoni, G.; Negri, F.; Vita Finzi, P.; Hussain, F.H.S.; Vidari, G. New tricholidic acid triterpenoids from the mushroom *Tricholoma ustaloides* collected in an Italian beech wood. *Molecules* **2023**, *28*, 3864. [CrossRef]
15. Nugroho, A.E.; Morita, H. Circular dichroism calculation for natural products. *J. Nat. Med.* **2014**, *68*, 1–10. [CrossRef] [PubMed]
16. Kirk, D.N. The chiroptical properties of carbonyl compounds. *Tetrahedron* **1986**, *42*, 777–818. [CrossRef]
17. Zhang, F.-L.; Feng, T. Diterpenes specially produced by fungi: Structures, biological activities, and biosynthesis (2010–2020). *J. Fungi* **2022**, *8*, 244. [CrossRef]
18. Breitmaier, E. Diterpenes. In *Terpenes: Flavors, Fragrances, Pharmaca, Pheromones*; Wiley-VCH: Berlin, Germany, 2006; Chapter 4; pp. 52–81. [CrossRef]
19. Gamba Invernizzi, A.; Vidari, G.; Vita Finzi, P. Trichoaurantianolide A, a new diterpene with an unprecedented carbon skeleton from *Tricholoma aurantium*. *Tetrahedron Lett.* **1995**, *36*, 1905–1908. [CrossRef]
20. Benevelli, F.; Carugo, O.; Gamba-Invernizzi, A.; Vidari, G. The structures of trichoaurantianolides B, C and D, Novel Diterpenes from *Tricholoma aurantium*. *Tetrahedron Lett.* **1995**, *36*, 3035–3038. [CrossRef]
21. Knops, L.; Nieger, M.; Steffan, B.; Steglich, W. Novel diterpenoids from the toadstools *T. aurantium* and *T. fracticum* (*Agaricales*). *Liebigs Ann.* **1995**, *1995*, 77–80. [CrossRef]
22. Williams, D.R.; Gladen, P.T.; Pinchman, J.R. Total synthesis of neodolastane trichoaurantanolides C and D. *J. Org. Chem.* **2015**, *80*, 5474–5493. [CrossRef]
23. Tsukamoto, S.; Macabalang, A.D.; Nakatani, K.; Obara, Y.; Nakahata, N.; Ohta, T. Tricholomalides A-C, new neurotrophic diterpenes from the mushroom *Tricholoma* sp. *J. Nat. Prod.* **2003**, *66*, 1578–1581. [CrossRef]
24. Wang, Z.; Min, S.-J.; Danishefsky, S.J. Total synthesis and structural revision of (±)-tricholomalides A and B. *J. Am. Chem. Soc.* **2009**, *131*, 10848–10849. [CrossRef]

25. Hiersemann, M.; Helmboldt, H. Recent Progress in the total synthesis of dolabellane and dolastane diterpenes. *Top. Curr. Chem.* **2005**, *243*, 73–136.
26. Corey, E.J.; Schmidt, G. Useful procedures for the oxidation of alcohols involving pyridinium dichromate in aprotic media. *Tetrahedron Lett.* **1979**, *20*, 399–402. [CrossRef]
27. Mazur, X.; Becker, U.; Anke, T.; Sterner, O. Two new bioactive diterpenes from *Lepista sordida*. *Phytochemistry* **1996**, *43*, 405–407. [CrossRef]